Dependence of the Electronic Properties of Hot-Wire CVD Amorphous Silicon-Germanium Alloys on Oxygen Impurity Levels

Shouvik Datta [1], J. David Cohen[1], Yueqin Xu [2], A.H. Mahan [2], and Howard M. Branz [2]

[1] Department of Physics, University of Oregon, Eugene, Oregon 97403,
[2] National Renewable Energy Laboratory, 1617 Cole Boulevard, Golden, CO 80401.

ABSTRACT

We report the effects of intentionally introducing up to ~ $5\times10^{20}/cm^3$ oxygen impurities into hydrogenated amorphous silicon-germanium alloys (of roughly 30at.% Ge) grown by the hot-wire chemical vapor deposition (HWCVD) method. Deep defect densities determined by drive-level capacitance profiling (DLCP) indicated a modest increase with increasing oxygen content (up to a factor of 3 at the highest oxygen level). Transient photocapacitance (TPC) spectra indicated a clear spectral signature for an optical transition between the valence band and an empty defect level, with an optical threshold around 1.3-1.4eV. This feature becomes stronger as the concentration of oxygen is increased. This transition results in a *negative* contribution to the TPC signal, and this initially led us to believe that the bandtail for the higher oxygen samples was much narrower than it actually is. Surprisingly, this additional oxygen related defect level appears to have only a very minor effect upon the estimated minority carrier collection fraction. The effects of light-induced degradation upon some of these oxygen contaminated samples were also examined in detail. We infer the existence of a significant thermal barrier to explain the observed spectral signature of this oxygen impurity defect.

INTRODUCTION

Electronic properties of a-Si,Ge:H alloys deposited by the hot-wire chemical vapor deposition (HWCVD) method have now improved to a level comparable to the best glow discharge (PECVD) a-Si,Ge:H alloy films. As was reported earlier [1- 6], these were obtained by replacing the usual tungsten filament with tantalum and using a filament temperature of ~1800°C instead of ~ 2000°C during the HWCVD growth process. We recently reported studies [5] in which we carried out a systematic incorporation of oxygen impurities for a series of a-Si,Ge:H alloy samples. Here we observed that the band tail actually appeared to become narrower as the oxygen content of a-Si,Ge:H films was increased. This seemed to suggest that the oxygen impurities actually improved the quality of these alloy films! However, a more detailed study was needed to understand the root cause of such oxygen induced electronic changes. Subsequently, these alloys were characterized using a variety of junction capacitance based techniques including transient photocapacitance (TPC) [7,8], transient photocurrent (TPI) spectroscopy, and drive-level capacitance profiling (DLCP) [9,10]. After careful analysis of these results, we now have a viable alternative explanation for the oxygen induced changes in a-Si,Ge:H alloys. Specifically, we believe our experimental results provide a clear signature of the optical excitation of valence band electrons into an empty oxygen related defect state. This results in a negative contribution to the TPC signal and accounts for many of the observed electronic changes in the oxygen rich a-$Si_{0.7}Ge_{0.3}$:H alloy films grown by HWCVD.

Table I. Oxygen concentrations and HWCVD growth parameters of a-$Si_{0.7}Ge_{0.3}$:H employed in this study. The tantalum filament temperature was about 1800°C.

Sample	Growth Rate (Å/s)	Air Leak Rate (sccm)	Thickness (microns)	Initial Substrate Temp (°C)	Final Substrate Temp (°C)	Oxygen concentrations (cm^{-3})
A	2.00	~0.00	1.80	204	289	$\sim 8\times10^{18}$
B	2.08	~0.02	1.75	204	289	$\sim 3\times10^{19}$
C	2.05	~0.06	1.60	204	284	$\sim 1\times10^{20}$
D	2.82	~0.20	2.20	204	275	$\sim 5\times10^{20}$

SAMPLES

A series of a-Si,Ge:H alloys with nominal Ge fractions around 30%, as determined by Secondary Ion Mass Spectrometry (SIMS), were deposited by the HWCVD technique at the National Renewable Energy Laboratory (NREL). These HWCVD depositions were carried out simultaneously on both stainless steel (SS) substrates and also on p^+ crystalline Si (c-Si) using a tantalum filament maintained at 1800°C. Oxygen levels were systematically varied using a controlled air leak into the growth chamber during the hot-wire CVD process. The SIMS measurements indicated a systematic increase of oxygen impurities (see Table I) as the air leak was gradually increased from sample A to sample D. At the same time, the nitrogen content was nearly identical and very low ($<4x10^{16}$ cm^{-3}). For the 30at.% Ge samples examined, gas ratios of $H_2/(SiH_4 + GeH_4) = 1$ and $GeH_4/(GeH_4 + SiH_4) = 0.19$ were utilized for all growth runs. Substrate temperatures were always set to 204°C at the beginning of film growth, but the final temperatures were higher (~280°C) due to heating by the HWCVD filament. Detailed growth parameters of the four samples examined in our current study are listed in Table I. Films were deposited simultaneously onto both specular stainless steel and on p^+ c-Si substrates. The silicon substrates are generally considered to be more reliable for the TPI measurements. Moreover, these samples allow us to examine the electronic properties of the a-Si,Ge:H material closer to the substrate where the properties were somewhat better due to the lower growth temperatures. Therefore, only the samples grown on c-silicon substrates will be discussed in this paper. A semi-transparent Pd contact was thermally evaporated on top of the intrinsic layer for junction capacitance based measurements. However, we utilized the reverse biased c-Si/a-Si,Ge:H depletion junction for all of the measurements described below.

CHARACTERIZATION METHODS

Drive Level Capacitance Profiling (DLCP) was used to determine deep defect density by fitting the non-linear capacitive response of the junction capacitance ($C = C_0 + C_1 \delta V + C_2 (\delta V)^2 + \ldots$) as a function of the amplitude, δV, of the applied oscillating voltage. The drive level density, N_{DL}, is then obtained from the coefficients C_0 and C_1 and it is directly related to an integral over the density of deep defect states near the spatial position $\langle x \rangle = \varepsilon A/C_0$ from the barrier junction. Thus we are able to obtain the portion of the deep defect band that responds at the measurement frequency and temperature. Spatial profiles of the deep defect densities were obtained by varying the dc reverse bias at each stage.

The transient photocapcitance (TPC) and transient photocurrent (TPI) techniques were used to obtain sub-band-gap optical absorption-like spectra. Unlike true absorption measurements, however, for these methods the signals result from the charge carriers that escape the depletion region in response to the absorbed photons. For TPC, optically excited changes in the junction capacitance indicate any change in the charge within the depletion width while, for the TPI technique, differences in the detected current as a result of optical excitation indicate the motion of the released charge. Thus, the TPC signal is sensitive to the *difference n-p*, where n and p are the number of (majority carrier) electrons and holes collected, respectively. However, the TPI signal is proportional to the *sum n+p* because the motion of either type of carrier produces a current of the same sign. As a result, when we compare these two types of spectra we can estimate the relative collection fraction of the minority carriers as p/n. [7,8]

EXPERIMENTAL RESULTS.

In Fig. 1 we plot the observed spatial profile of deep defect densities as measured by DLCP technique. We see that the deep defect density in the annealed State A increases from a value ~7×10^{15}/cm^3 in sample A (lowest oxygen) to ~2×10^{16}/cm^3 in sample D (highest oxygen). These samples were also examined in a degraded State B produced by light soaking for 100 hours at roughly 1W/cm^2 intensity using a ELH source with a 610nm long pass filter. The deep defect densities of the samples with different oxygen contents, did increase somewhat, although less than a factor of 2 in all cases.

Figure 2 shows the TPC and TPI spectra of sample C (10^{20} cm^{-3} oxygen) in both State A and State B. Our initial analysis noted that the TPC spectra appeared to indicate that this sample has an extremely narrow bandtail, with an Urbach energy below 40meV.[5] However, a very different picture emerges when analyzing both the TPC and TPI spectra together. The thin solid lines shown in Fig. 2 indicate that quite a good fit can be obtained. However, these fits require that we include an additional band of transitions, from the valence band to a defect with an optical threshold centered at ~1.35 to ~1.4eV. Because this transition predominantly results in the release of a hole instead of an electron, they contribute *negatively* to TPC spectrum and *positively* to the TPI spectrum. It is this negative contribution to the TPC signal that makes its

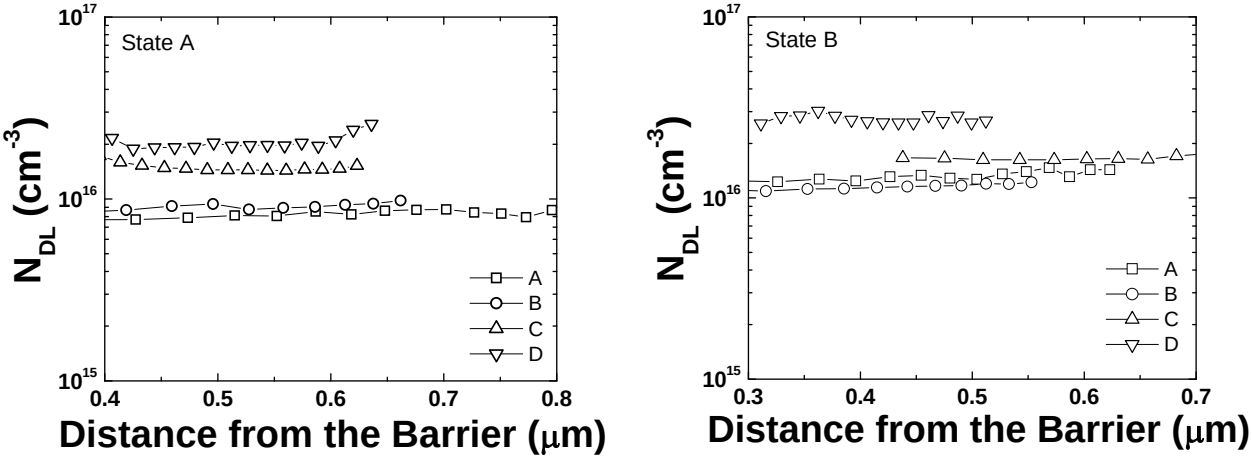

FIG. 1. Spatial Profile of deep defect density in (a) the annealed State A and (b) in the light-soaked State B. These DLC profiles were obtained at 1.1 kHz and 370K.

bandtail appear unusually narrow. In actual fact, however, the correct Urbach energy as obtained from these fits is close to 47meV. Also, from the ratio of the TPI and TPC magnitudes in the upper portion of the bandtail region we can deduce the relative hole collection fractions for this sample. It is ~96% for this sample in State A, with perhaps even a slight increase in State B. This appears to exceed the hole collection fraction determined for the best PECVD a-Si,Ge:H in this alloy range.

Figure 3 exhibits a comparison of the TPC spectra for three samples with increasing oxygen levels. We see that the 1.4eV transition is basically absent from the spectrum of the sample with no intentional oxygen incorporation during the HWCVD growth, and increases with as the oxygen level increases. We thus attribute this 2nd defect band with the oxygen impurities

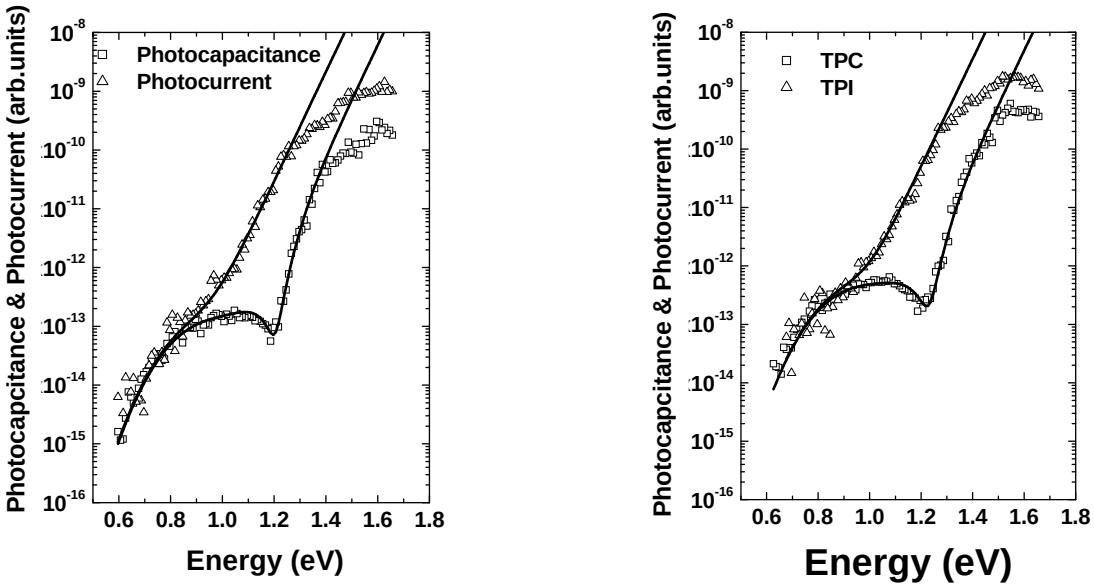

FIG. 2. Photocapacitance and Photocurrent spectra for the a-$Si_{0.7}Ge_{0.3}$:H sample C with ~$1\times10^{20}/cm^3$ oxygen in (a) its annealed State, and (b) a light-soaked state. The thin solid lines are fits assuming 47meV Urbach tail plus a transition from a filled defect with an optical threshold of ~0.84eV below E_C, plus a second deep defect transition with an optical threshold roughly 1.4eV above E_V.

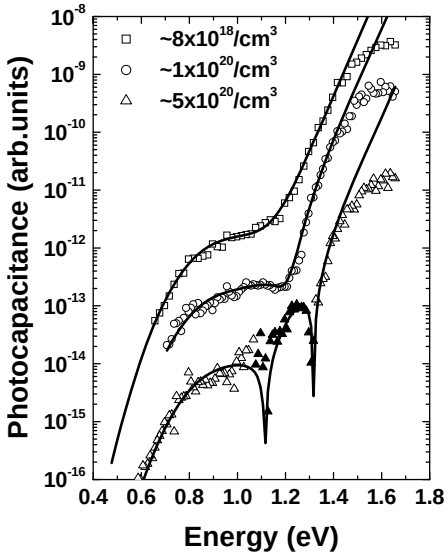

FIG. 3. Photocapacitance spectra for three a-$Si_{0.7}Ge_{0.3}$:H samples with different oxygen levels. The thin solid lines indicate fits obtained in the same manner as those in Fig. 2. In the case of fitting the spectrum for the sample without intentional oxygen contamination, the 2nd defect transition at ~1.4eV above the valence was negligible. Also, for that sample the Urbach energy was 45meV, and was 47meV for the other two samples. For the sample with highest oxygen content, the TPC signal actually became *negative* (filled triangles) for the region between 1.1 and 1.4eV.

present in these a-$Si_{0.7}Ge_{0.3}$:H alloy films. However, this increased oxygen level appears to have only a very minor effect upon the minority carrier collection fraction. For the lowest oxygen sample we deduce an Urbach energy of 45meV, among the lowest ever measured for a a-Si,Ge:H sample in this alloy range. Correspondingly, the relative collection fraction of hole-to electron was found to be around 97% for that sample. Moreover, as indicated in Figs. 1 and 2, these HWCVD deposited a-Si,Ge:H films appear to be much more stable with respect to light-induced degradation than the highest quality PECVD a-Si,Ge:H samples studied [5,6] previously by these methods. However, this may partially be because their initial deep defect densities are close to 10^{16} cm^{-3}, compared to the mid 10^{15} cm^{-3} level of those previous PECVD samples.

One interesting remaining issue concerns why the transition into an empty defect band at ~1.4eV from the valence band should be so predominantly negative for sample D. This can only be possible if the electron that is inserted from the valence band remains strongly trapped for the duration of the measurement time window (of roughly 0.4s). We attempted to study the subsequent thermal emission of this trapped electron by recording the TPC spectra for the highest oxygen doped sample over a wider range of temperatures. Three such spectra are shown in Fig. 4 and, in Fig. 5, we plot the temperature dependence of the TPC signal at a photon energy of 1.2eV (where the signal due to the 1.4eV transition is clearly visible and is also less obscured by the bandtail signal). This temperature dependence indicates that the (negative) contribution due to the oxygen impurity peaks near 370K. Moreover, above ~380K, the photocapacitance signal is reduced in magnitude due to the subsequent thermal emission of this optically trapped electron from this 2nd defect state. Also, below about 345K the TPC signal increases monotonically to a large positive value. We believe this is due to an increasing positive contribution from the bandtail which is always found to become significantly larger at lower temperatures as also shown in Fig. 5.

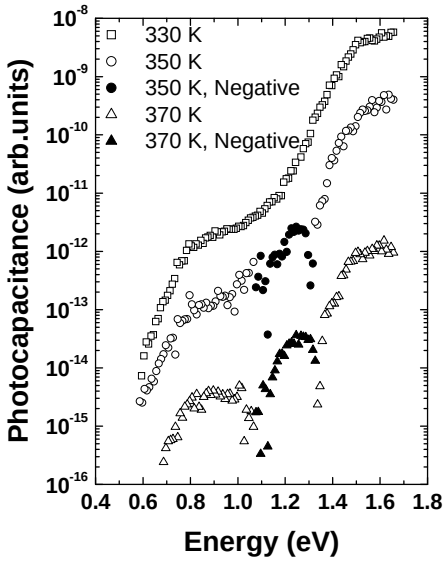

FIG. 4. TPC spectra of the highest oxygen a-Si,Ge:H sample at 3 temperatures. These spectra were been vertically shifted from each other for greater visibility. Note the relative increase of the negative feature (filled symbols) near 1.2eV at higher temperatures, and the relative decrease in the bandtail signal.

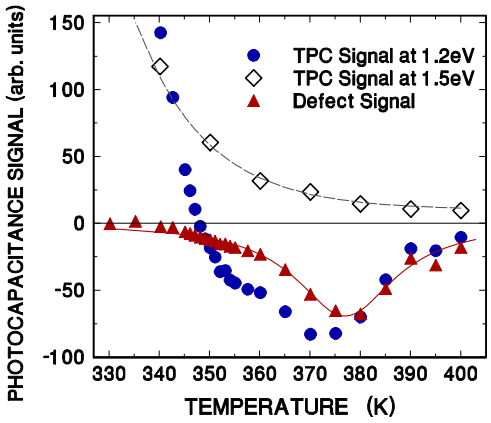

FIG. 5. Temperature variation of the TPC signal at photon energies near 1.2 eV (circles) and 1.5eV (diamonds). We have attempted to deduce the underlying temperature dependence of the oxygen related defect signal (triangles) by first normalizing the 1.2eV response to the near bandgap 1.5eV response, and then subtracting off a portion of the bandtail signal to correct for its contribution at 1.2eV that becomes significant at lower temperatures.

DISCUSSION

Based on our experimental results, we hypothesize that the observed oxygen impurity related defect state is associated with a positively charged oxygen donor level, possibly that previously suggested three fold coordinated (O_3^+) type centers in a-Si:H [11- 14]. The 1.4eV transition energy from the valence band indicates a center close to the conduction band; however, to account for the observed behavior, it is also necessary that in the O_3^0 state, the trapped electron cannot be thermally emitted into the conduction band very quickly. This clearly requires the presence of a significant thermal barrier to inhibit this. We hope that additional junction capacitance experiments that are currently in progress will be able to map oout a more complete configurational relaxation diagram for the optically induced electron capture by this oxygen related defect in these HWCVD grown a-Si,Ge:H alloys.

ACKNOWLEDGEMENTS

Work at the University of Oregon was supported by NREL Subcontract ZXL-5-44205-11. Work at NREL was supported by the U.S. DOE under Contract DE-AC36-99GO10337.

REFERENCES

1. Y. Xu, B. P. Nelson, D. L. Willamson, L. M. Gedvilas, and R.C. Reedy, Mat. Res. Soc. Symp. Proc. **762**, A10.2 (2003).
2. D.L. Williamson, G. Goerigk, Y. Xu, and A.H. Mahan, Proceedings DOE Solar Energy Technologies Review Meeting, DOE/GO-102005-2067 (2005) p. 444.
3. S. Datta, J. D. Cohen, Y.Xu, and A. H. Mahan, Mat. Res. Soc. Symp. Proc. **862**, A7.2 (2005).
4. Shouvik Datta, Yueqin Xu, A. H. Mahan, Howard M. Branz, and J. David Cohen, J of Non-Cryst Solid, **352**,1250 (2006).
5. Shouvik Datta, J David Cohen, Steve Golledge, Yueqin Xu, A. H. Mahan, James R. Doyle and Howard M. Branz, Mat. Res. Soc. Symp. Proc **910**, A2.5 (2006).
6. J.D. Cohen, S. Datta, K. Palinginis, A.H. Mahan, E. Iwaniczko, Y. Xu, and H.M. Branz. Thin Solid Films (in press).
7. A.V. Gelatos, K.K. Mahavadi, J.D. Cohen, and J.P. Harbison, Appl. Phys. Lett. **53**, 403 (1988).
8. J. David Cohen and Avgerinos V. Gelatos, in *Amorphous Silicon and Related Materials*, Vol. A, ed. by Hellmut Fritzsche (World Scientific, Singapore, 1989), p 475.
9. C. E. Michelson, A. V. Gelatos, and J. D. Cohen, Appl. Phys. Lett. **47**, 412 (1985).
10. J. David Cohen and Avgerinos V. Gelatos, in Amorphous Silicon and Related Materials, edited by Hellmut Fritzsche Vol A (World Scientific, Singapore, 1989), p 475.
11. R. A. Street and N. F. Mott, Phys. Rev. Lett. **35**, 1293 (1975).
12. David Adler, Solar cells. **9**, 133 (1983).
13. Tatsuo Shimizu, Minoru Matsumoto, Masahiro Yoshita, Masahiko Iwami, Akiharu Morimoto, and Minoru Kumeda, J. Non-Cryst. Solids. **137&138**, 391 (1991).
14. H. Fritzsche, J. Non-Cryst. Solids. **190**, 180 (1995).